STUDY OF COULOMB NUCLEAR INTERFERENCE IN ^{12}N NUCLEUS BREAKUP REACTION

Surender Kaliraman, Ravinder Kumar
Department of Physics, Deenbandhu Chhotu Ram University of Science and Technology, Murthal (Sonipat), Haryana, IN-131 039, India

(Received 19 December 2024; in final form 24 February 2025; accepted 09 March 2025; published online 18 June 2025)

We investigated the Coulomb-nuclear interference effect on a single proton removal cross-section and full width at half maximum (FWHM) of longitudinal momentum distribution (LMD) in the breakup reaction of a proton rich ^{12}N nucleus. The effect is analyzed for three different targets: ^{12}C, ^{58}Ni and ^{208}Pb nucleus, in 40–100 MeV/u incident beam energy range. The Coulomb breakup mechanism is treated with all-order sudden approximation, while the nuclear breakup, including both stripping and diffraction is treated using eikonal approximation. The obtained results show that the interference among breakup mechanisms significantly affects the single proton breakup cross-section, more specifically in medium-mass target cases. However, the effect is found to be below 6% for FWHM of LMD for all the chosen targets. The obtained results show that in medium-mass targets reactions, it is crucial to consider the interference between the Coulomb and diffraction breakup processes for 40–100 MeV/u energies. We believe that this understanding of the obtained results will be valuable for planning future experiments involving proton halo nuclei and also add better clarity in the interpretation of experimental results.

Key words: Halo Nuclei, breakup reaction, interference effect, one proton removal cross-section.

DOI: https://doi.org/10.30970/jps.29.2201

I. INTRODUCTION

With advancements in radioactive ion beams (RIB) in nuclear physics, the discovery of new exotic nuclei has become more accessible. These radioactive nuclei exhibit intriguing characteristics, such as a short lifetime, large nuclear size, a large matter distribution, a novel shell structure, new excited states and decay patterns. One common feature of these nuclei is their small one-particle separation energy, often around 1 MeV or less. This small separation energy among neutron- or proton-rich nuclei leads to a variety of characteristics, including soft collective modes, unusual transition strengths between low-lying states, changes in nuclear shell structure and extended density distribution, and forms a halo nuclear structure.

Halo nuclei possess an extended matter density distribution, where one or two nucleons (proton or neutron) lie far from the compact nuclear core. Frequently, the single nucleon removal reactions are used to reveal their nuclear structure. In single nucleon removal reactions, the width of longitudinal momentum distributions of the core fragment is unusually measured narrower in comparison to the normal stable nuclei, which indicates an increased nuclear size, which is duly reflected in their large total reaction and breakup cross-section. Such nuclei were initially termed "halo nuclei" by Tanihata in 1985 [1, 2].

Among these exotic nuclei, single neutron halos are more commonly observed than those of single valence proton halos, that is because of the presence of the Coulomb barrier, which prevents the valence proton from extending far into the forbidden region. So proton halos are rare in comparison to the neutron halos; besides, there are many proton halos which lie near the proton drip line. Since their discovery, the study of the proton halo structure has been a fascinating area of nuclear research. Additionally, recent observations of spontaneous two-proton radioactivity near the proton drip line further highlight the unique behavior of these exotic systems. A few investigations indicated the existence of a single proton halo structure in proton-rich nuclei ^{8}B [3–7], ^{17}Ne, and $^{26-29}$P [8–10], ^{23}Al [11–15],^{17}F [16]. In proton halo nuclei studies, the measurement of LMD of the core fragment and single proton breakup cross-section has been the key observables used to reveal their structure features and, consequently has been used to reliably estimate the nuclear reaction rate taking place in nucleosynthesis reactions in stars and supernovas [17–20]. Hence, it is crucial to understand precisely their sensitivity to the atomic number of the target nucleus, incident beam energy, and also to the interference in breakup mechanisms. In halo breakup reactions, the breakup occurs due to nuclear and Coulomb repulsive interactions between the projectile and target nuclei. The nuclear breakup mechanism dominates during the interactions with light target nuclei (light atomic number) at low impact parameters, typically less than or equal to the sum of the root mean square (RMS) radii of the target and projectile while the Coulomb breakup occurs due to the Coulomb repulsive interaction between the projectile and target nuclei, and dominates in the case of heavy targets (high atomic number) at high impact parameters (more than the sum of the root mean square (RMS) radii of the target and projectile). But during the breakup, it is too difficult to say which mechanism is causing the breakup, especially near the surface region. Both the Coulomb and nuclear breakup mechanism equally work together and cause the breakup of the valence nucleon from the projectile nucleus, so it is difficult to separate and estimate the absolute magnitude of each breakup observable corresponding to each breakup mechanism.

So far numerous papers have been published for proton halos and neutron halos with different targets [21–26]

etc. They reported that both interactions occur simultaneously, especially near the surface region, and lead to the possibility of interference between the Coulomb and nuclear diffraction mechanism, which can affect the observables of the breakup reaction. A substantial number of articles highlight that interference in breakup mechanism is a crucial phenomenon and always remains present in breakup reactions which significantly affect the absolute magnitudes of breakup observables. [16, 27–34]. So underestimation of this interference may lead to large ambiguity in the interpretation of experimental results and, consequently, can be misleading in understanding of these exotic nuclei of astrophysical interest. Also, in proton halo Coulomb breakup reactions, the total Coulomb breakup interactions consist of two types of interactions, i.e. the Coulomb interaction between the projectile's valence proton and target nucleus (called Direct Coulomb interaction) and the Coulomb interaction between the core of the projectile and the target nucleus (called Recoil Coulomb interaction). A few recent works have focused directly on these two interferences among breakup mechanisms [16, 27–34], showing that the interference effect plays a significant role: many time they show constructive nature and many times destructive nature, depending on the target nucleus atomic number and incident beam energy. Being motivated by these works, in the present work we investigated the presence of both kinds of interference in the breakup of a proton rich ^{12}N nucleus. We perform a quantitative investigation showing the effect of interference on the magnitude of a single proton breakup cross-section and LMD width. The sensitivity of this effect has been analyzed for light, medium, and heavy target nuclei in a medium energy range, in which mostly experiments are performed, i. e. 40–100 MeV/u.

The ^{12}N nucleus is of paramount interest to nuclear physicists due to its unique properties. This nucleus has an unusual proton to neutron ratio and extremely short half-lives of about milliseconds, which provide crucial insights into the behavior of the nuclear matter under extreme conditions. Understanding such nuclear structure, its decay modes and production mechanisms is pivotal in advancing our knowledge of nuclear physics. Additionally, exotic nuclei, including ^{12}N, play a significant role in understanding the nucleosynthesis reactions taking place in stars and supernovaes [17]. The ^{12}N study is essential because it has small proton separation energy $S_p = 0.6$ MeV, and it has a large reaction cross-section and a large single proton removal cross-section [17–20, 35, 36]. Moreover, the proton removal process from ^{12}N nucleus is related to the ^{11}C$+p$ radiative capture reaction depending on the initial CNO abundances. This reaction might have played a significant role in some supermassive stars in the early universe, allowing these stars to explode as supernovae, rather than collapsing into black holes without ejecting any mass [37–44] . Also, recently the asymptotic normalisation coefficient (ANC) for $^{12}\mathrm{N} \rightarrow {}^{11}\mathrm{C} + p$ has been measured using transfer reactions [18]. The calculation of the ANC via a breakup reaction was being used to obtain the reaction rate data but could not be achieved correctly [19, 20]. Therefore, keeping in view the importance of this breakup reaction, we studied the breakup reaction of the ^{12}N nucleus with different targets i.e. ^{12}C, ^{58}Ni, and ^{208}Pb in 40–100 MeV/n incident beam energy range and tried to understand the effects of the Coulomb nuclear interference on the absolute magnitude of a single proton breakup cross-section and FWHM width of LMD. The paper is arranged as follows: section II discusses the theoretical formalism, section III discusses the obtained results, and finally, section IV presents the conclusions.

II. THEORETICAL FORMALISM

We followed the theoretical formalism of [16, 28–32, 45], where the Coulomb potential between the projectile and target causing the breakup of a projectile nucleus is defined as:

$$V(\mathbf{r},\mathbf{R}) = \frac{V_\mathrm{c}}{\mid \mathbf{R} - \beta_1 \mathbf{r} \mid} + \frac{V_\mathrm{v}}{\mid \mathbf{R} + \beta_2 \mathbf{r} \mid} - \frac{V_0}{\mathbf{R}}. \quad (1)$$

Here, (Z_c), (Z_t), and (Z_v) represent the core, target, and valence proton charges, respectively. $(V_\mathrm{c} = Z_\mathrm{c} Z_\mathrm{t} e^2)$, $(V_\mathrm{v} = Z_\mathrm{v} Z_\mathrm{t} e^2)$, and $(V_0 = (Z_\mathrm{v} + Z_\mathrm{c})\, Z_\mathrm{t} e^2$ are the Coulomb potential between core and target, valence proton and target, and whole projectile and target respectively. The β_1 and β_2 are the mass ratios of proton and core to the projectile mass. The $\mathbf{r}$ and $\mathbf{R}$ are position vectors representing the core-to-proton and target-to-projectile centre of mass distances, as shown in Fig. 1 (taken from [30]). The centre of mass of the projectile is assumed to follow a straight line, $\mathbf{R} = \hat{x} R_\perp + \hat{z} vt$, where v is the relative motion velocity at the distance of closest approach.

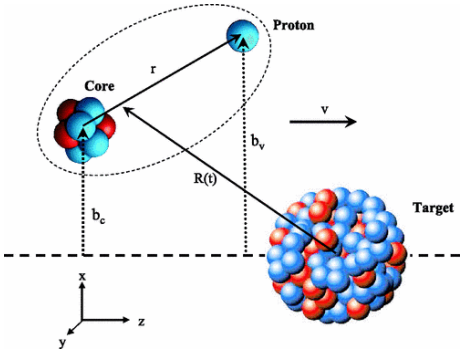

Fig. 1. Geometry of the coordinate system used for the projectile-target interaction [30]

Using the perturbative procedure, discussed in detail in Ref. [28], the Coulomb phase can be defined for proton halo breakup as:

$$\chi_\mathrm{pert} = \frac{1}{\hbar} \int dt\, e^{i\omega t} V(\mathbf{r}, t). \quad (2)$$

The perturbed Coulomb phase for the entire two body proton halo projectile (comprising of core and valence

proton) is given by [28, 29]:

$$\chi^{\rm p} = \frac{2}{\hbar v}\Big(V_{\rm c}e^{i\beta_1\omega z/v}K_0(\omega b_{\rm c}/v) - V_0K_0(\omega R_\perp/v) + V_{\rm v}e^{-i\beta_2\omega z/v}K_0(\omega b_{\rm v}/v)\Big), \quad (3)$$

where $\omega = (\varepsilon_{\rm f} - \varepsilon_0)/\hbar$, with ε_0 representing the valence nucleon binding energy and $\varepsilon_{\rm f}$ the final nucleon-core continuum energy, K_0 is the modified Bessel function, v is the velocity of the projectile, and $b_{\rm c}$ and $b_{\rm v}$ are core and valence proton impact parameters. The whole projectile Coulomb potential (V_0) can be expressed as the sum of the core ($V_{\rm c}$) — target Coulomb potential and the valence proton ($V_{\rm v}$) — target Coulomb potentials, i. e., $V_0 = V_{\rm c} + V_{\rm v}$. Thus, the entire projectile's perturbed Coulomb phase can be written as:

$$\chi^{\rm p} = \chi(\beta_1, V_{\rm c}) + \chi(-\beta_2, V_{\rm v}). \quad (4)$$

where the term $\chi(\beta_1, V_{\rm c})$ is called the Recoil Coulomb phase which appears due to Coulomb repulsion between the core and the target, whereas other $\chi(-\beta_2, V_{\rm v})$ is called the Direct proton target Coulomb phase due to the valence proton target Coulomb interaction and can separately be written as [29].

$$\chi(\beta_1, V_{\rm c}) = \frac{2V_{\rm c}}{\hbar v}\left(e^{i\beta_1\omega z/v}K_0(\omega b_{\rm c}/v) - K_0(\omega R_\perp/v)\right), \quad (5)$$

$$\chi(-\beta_2, V_{\rm v}) = \frac{2V_{\rm v}}{\hbar v}\left(e^{-i\beta_2\omega z/v}K_0(\omega b_{\rm v}/v) - K_0(\omega R_\perp/v)\right). \quad (6)$$

So far numerous theoretical studies have emphasized the importance of including the Coulomb breakup mechanisms in all orders including all multipoles of the Coulomb potential, especially in proton halo breakup reactions [16, 30, 46]. Therefore, we have treated each Coulomb interaction to all orders with the time dependent perturbation theory and sudden formalism [45]. The all-order theoretical formalism is discussed in full detail in [16, 28–30, 46–48], and so the Coulomb breakup probability amplitudes are:

$$g^{\rm rec}(b_c) = \int d\mathbf{r}\, e^{-i\mathbf{k}\cdot\mathbf{r}}\phi_i(\mathbf{r})\left(e^{i\frac{2V_{\rm c}}{\hbar v}\log\frac{b_{\rm c}}{R_\perp}} - 1 - i\frac{2V_{\rm c}}{\hbar v}\log\frac{b_{\rm c}}{R_\perp} + i\chi(\beta_1, V_{\rm c})\right), \quad (7)$$

$$g^{\rm dir}(b_v) = \int d\mathbf{r}\, e^{-i\mathbf{k}\cdot\mathbf{r}}\phi_i(\mathbf{r})\left(e^{i\frac{2V_{\rm v}}{\hbar v}\log\frac{b_{\rm v}}{R_\perp}} - 1 - i\frac{2V_{\rm v}}{\hbar v}\log\frac{b_{\rm v}}{R_\perp} + i\chi(-\beta_2, V_{\rm v})\right). \quad (8)$$

While the nuclear diffraction dissociation amplitude within the eikonal approximation is well know by

$$g^{\rm diff}(b_v) = \int d\mathbf{r}\, e^{-i\mathbf{k}\cdot\mathbf{r}}\phi_i(\mathbf{r})\left(e^{i\chi_{\rm nt}(b_{\rm v})} - 1\right), \quad (9)$$

the core fragment momentum distribution containing nuclear diffraction and total Coulomb (recoil and direct) amplitudes can be expressed as:

$$\frac{d\sigma}{d\mathbf{k}_z} = \frac{1}{8\pi^3}\int d\mathbf{b}_{\rm c}\,|S_{\rm ct}(b_{\rm c})|^2|g^{\rm rec} + g^{\rm dir} + g^{\rm diff}|^2. \quad (10)$$

So the core fragment LMD is obtained by integrating the core fragment momentum distribution (10) over its transverse component of momentum and the single proton breakup cross-section is then obtained by integrating the LMD spectrum over the momentum, respectively. Here, ($S_{\rm ct}(b_{\rm c})$) and ($e^{i\chi_{\rm nt}(b_{\rm v})}$) are core–target and proton–target S-matrices or profile functions, which are obtained using Hartree–Fock nuclear density forms [49–51] of core and target nuclei, using the t-$\rho\rho$ method with the standard MOMDIS code [52]. The projectile wave function ϕ_i of ground state of projectile [$3/2^+ \otimes 1p_{3/2}$] is calculated numerically by solving the Schrödinger wave equation using the Woods–Saxon nuclear potential. The depth of WS nuclear potential ($V_0 = 37.13$ MeV) is adjusted to fit the proton separation energy ($S_p^{\rm eff} = 0.6$ MeV) with the range and diffuseness parameter $r_0 = 1.27$ fm, $a_0 = 0.7$ fm. In the present study, to examine the presence of interference between the Coulomb and nuclear diffraction mechanisms, we first treat nuclear diffraction and Coulomb breakup processes as independent, calculating observables in the absence of each other. Conversely, we also calculate observables in the presence of both mechanisms to analyze their combined effect.

Here, the quantitative effect of the Coulomb nuclear diffraction interference on the absolute magnitude of breakup observables is obtained in terms of percent variation using the following formula, so the obtained values are shown in respective tables.

$$\%\text{Interference} = \frac{X^{\text{Coul + Diff}} - \left(X^{\text{Coul}} + X^{\text{Diff}}\right)}{\left(X^{\text{Coul}} + X^{\text{Diff}}\right)} \times 100. \tag{11}$$

Similarly, the percent effect of the interference between the Recoil and Direct Coulomb mechanismes is obtained using the formula:

$$\%\text{Interference} = \frac{X^{\text{Coul (Recoil + Direct)}} - \left(X^{\text{Recoil}} + X^{\text{Direct}}\right)}{\left(X^{\text{Recoil}} + X^{\text{Direct}}\right)} \times 100, \tag{12}$$

where the notation X is a dummy symbol to represent single proton breakup cross-section (σ_{-p}) or FWHM of LMD. $X^{\text{Coul+Diff}}$ stand for the Coulomb and diffraction calculated together in the presence of both mechanisms, while X^{Coul} or X^{Diff} are independent mechanisms calculated in the absence of the other mechanism. Similarly, in other $X^{\text{Coul(Recoil+Direct)}}$ contains both *Direct* and *Recoil* Coulomb interactions, while X^{Direct} or X^{Recoil} are independent interactions.

III. RESULTS AND DISCUSSION

In this study, we investigated the single proton breakup from ^{12}N nucleus with three different target nuclei. We analyzed the effect of the Coulomb nuclear diffraction interference on the key breakup observables, for three distinct targets, i. e. ^{12}C, ^{58}Ni, and ^{208}Pb (frequently used in breakup reactions), at 40, 60, 80 and 100 MeV/u incident beam energy. To simplify the analysis and for a general understanding of the reaction phenomenon, we simply used the frequently reported projectile state, having core plus valence proton configuration $[3/2^+ \otimes 1p_{3/2}]$. Using the above discussed theoretical formalism, single proton breakup cross sections and LMD widths are calculated and their absolute magnitudes are shown in tables. Tables 1, 3, and 5 present the calculated single proton breakup cross-sections, while Tables 2, 4, and 6 shows the FWHM of LMD. Each table show exclusively the calculated magnitude of breakup observables, breakup mechanisms wise, where Nuclear Diffraction is referred to as "Diffraction", total Coulomb is referred to as "Coulomb", the simple sum of Coulomb and Nuclear Diffraction in the absence of each other are referred to as "Coul + Diff (simple sum)", and Coulomb and Diffraction calculated together in the presence of both mechanisms are referred to as "Coul + Diff (cal. togh.)". Also, the interference between the Direct and Recoil Coulomb mechanisms and consequently its effect on the magnitude of observable are shown on the lower sections of each table, where Recoil Coulomb breakup is referred to as "Recoil", Direct Coulomb breakup is referred to as "Direct", the simple algebraic sum of Recoil and Direct contributions is referred to as "Recoil + Direct (simple sum)", while the contribution in the presence of both Recoil and Direct mechanism is referred to as "Recoil + Direct (cal. togh.)

Beam Energy →	40 MeV/u	60 MeV/u	80 MeV/u	100 MeV/u
Breakup Mechanism	σ_{-p} (mb)	σ_{-p} (mb)	σ_{-p} (mb)	σ_{-p} (mb)
Diffraction	42.46	62.66	47.06	29.05
Coulomb	10.20	7.85	5.83	5.44
Coul + Diff (simple sum)	52.66	70.51	53.41	34.50
Coul + Diff (cal. togh.)	54.25	68.11	49.43	30.84
% Interference	+3.03	−3.40	−7.45	−10.61
Recoil	7.85	6.37	4.96	4.67
Direct	30.27	24.33	18.88	17.66
Recoil + Direct (simple sum)	38.13	30.70	23.84	22.33
Recoil + Direct (cal. togh.)	10.20	7.85	5.83	5.44
% Interference	−73.25	−74.44	−75.54	−75.64

Table 1. Calculated single proton breakup cross-section (σ_{-p} in mb) for ^{12}N projectile on ^{12}C target at different incident beam energies corresponding to diffraction, Coulomb, and diffraction with Coulomb mechanisms, along with their percentage interference effects

Beam Energy →	40 MeV/u	60 MeV/u	80 MeV/u	100 MeV/u
Breakup Mechanism	FWHM (MeV/c)	FWHM (MeV/c)	FWHM (MeV/c)	FWHM (MeV/c)
Diffraction	104.75	110.40	110.09	110.69
Coulomb	72.38	74.18	72.73	75.36
Coul + Diff (simple sum)	94.27	103.11	102.78	101.21
Coul + Diff (cal. togh.)	93.90	102.39	102.66	101.65
% Interference	−0.39	−0.69	−0.11	+0.43
Recoil	56.04	58.94	59.43	61.82
Direct	60.85	63.62	63.52	66.01
Recoil + Direct (simple sum)	59.63	62.44	62.46	64.94
Recoil + Direct (cal. togh.)	72.38	74.18	72.73	75.36
% Interference	+21.38	+18.80	+16.44	+16.04

Table 2. Calculated FWHM of LMD (MeV/c) for ^{12}N projectile on ^{12}C target at different incident beam energies corresponding to diffraction, Coulomb, and diffraction with Coulomb mechanisms, along with their percentage interference effects

Beam Energy →	40 MeV/u	60 MeV/u	80 MeV/u	100 MeV/u
Breakup Mechanism	σ_{-p} (mb)	σ_{-p} (mb)	σ_{-p} (mb)	σ_{-p} (mb)
Diffraction	18.83	25.20	23.71	20.87
Coulomb	200.54	144.89	117.81	100.37
Coul + Diff (simple sum)	219.37	170.09	141.52	121.24
Coul + Diff (cal. togh.)	256.71	203.51	169.18	144.46
% Interference	+17.02	+19.65	+19.54	+19.15
Recoil	133.63	109.45	94.74	84.08
Direct	489.99	400.90	347.11	307.99
Recoil + Direct (simple sum)	623.63	510.35	441.85	392.07
Recoil + Direct (cal. togh.)	200.54	144.89	117.81	100.37
% Interference	−67.84	−71.61	−73.34	−74.39

Table 3. Calculated single proton breakup cross-section (σ_{-p} in mb) for ^{12}N projectile on ^{58}Ni target at different incident beam energies corresponding to diffraction, Coulomb, and diffraction with Coulomb mechanisms, along with their percentage interference effects

Beam Energy →	40 MeV/u	60 MeV/u	80 MeV/u	100 MeV/u
Breakup Mechanism	FWHM (MeV/c)	FWHM (MeV/c)	FWHM (MeV/c)	FWHM (MeV/c)
Diffraction	82.44	86.88	87.34	86.56
Coulomb	67.37	68.43	69.50	70.19
Coul + Diff (simple sum)	68.35	70.24	71.49	72.13
Coul + Diff (cal. togh.)	71.90	73.17	73.88	74.22
% Interference	+5.19	+4.17	+3.34	+2.77
Recoil	53.50	56.02	58.18	59.77
Direct	56.70	59.27	61.35	62.80
Recoil + Direct (simple sum)	55.87	58.45	60.44	61.93
Recoil + Direct (cal. togh.)	67.37	68.43	69.50	70.19
% Interference	+20.58	+17.07	+14.99	+13.34

Table 4. Calculated FWHM of LMD (MeV/c) for ^{12}N projectile on ^{58}Ni target at different incident beam energies corresponding to diffraction, Coulomb, and diffraction with Coulomb mechanisms, along with their percentage interference effects

Tables 1 and 2 show respectively the calculated single proton breakup cross-section and FWHM width of LMD in the case of ^{12}C target at 40–100 MeV/u incident beam energies. It can be seen from Table 1 that due to the small size (low atomic number) of the target, nuclear breakup mechanism is predominant over the Coulomb breakup and hence showing larger cross-section for each incident energy, while the Coulomb mechanism contribution is small and it decreases with incident energy.

At 40 MeV/u, the percentage change in the single proton breakup cross-section due to interference between Coulomb and nuclear diffraction is of constructive nature, which enhances the magnitude of cross-section by 3%. However, as the beam energy increases from 60 to 100 MeV/u, the interference shows destructive character, which suppresses the single proton breakup cross-section from 3% to 10%. Also, this destructiveness increases with incident energy. But, on the other hand, the percentage change in the FWHM of LMD is observed negligibly smaller than 1%, and it is insensitive to the incident energy as can be seen from Table 2.

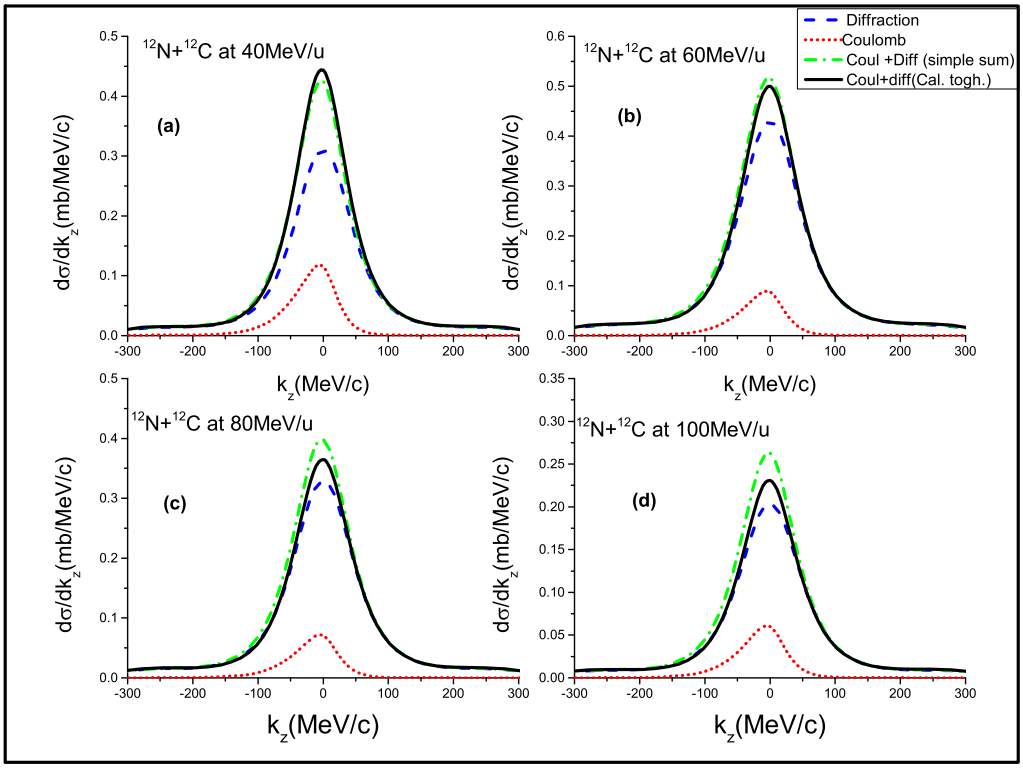

Fig. 2. LMD spectrum of the core fragment in the case of ^{12}C target at different incident energies showing the effect of the Coulomb nuclear diffraction interference. In each figure the red dotted curve corresponds to the total Coulomb mechanism, the blue dashed curve corresponds to the Diffraction mechanism, the green dash-dotted curve corresponds to a simple sum of the Coulomb and Diffraction mechanisms, and the solid black curve corresponds to the combined the Coulomb and Diffraction mechanism

In addition, the interference between Recoil and Direct Coulomb breakup mechanism is of destructive nature, which reduces the breakup cross-section around 73–75% and is almost insensitive to the beam energy. Conversely, the FWHM of the LMD shows a constructive nature, which enhances the LMD width from 21% to 16%, but this enhancement decreases with incident energy. For better clarity, the breakup mechanism wise LMD spectrums are shown in Figs. 2 and 3.

Tables 3 and 4 give the breakup cross-section and FWHM of LMD for the ^{58}Ni target at the beam energy from 40 to 100 MeV/u. From Table 3, we find that the total breakup cross-section is increased by 17 to 20% and is constructive due to the interference effect between the Coulomb and nuclear diffraction. However, the percentage change in FWHM of LMD distribution is less constructive in nature and varies from 2–5%. If we look at the lower part of both tables, the percentage change in the total Coulomb is destructive due to the interference effect in Recoil and Direct Coulomb. It reduces the breakup cross-section from 67 to 74%, but FWHM is increasing due to this interference in the range of 13–20%, which is constructive. Here we find that interference is high because both Coulomb and nuclear diffraction breakup can dominate; these results are similar to our recent findings [46]. Figures 4 and 5 show the LMD, and each line has its usual meaning, like Figs. 2 and 3, respectively.

In Fig. 4, we found that due to the interference of the Coulomb and nuclear diffraction mechanism, the black solid curve [Coul+diff(cal.tog)] is bigger than the green dashed curve [Cou+diff(simple sum)], for all the incident energies, and reflecting the constructive nature of the interference. However, the interference between direct and Recoil Coulomb mechanism is found always destructive, because of which the total Coulomb (black curve) mechanism curve is always smaller than that of a simple sum of direct and Recoil curve(green dash curve).

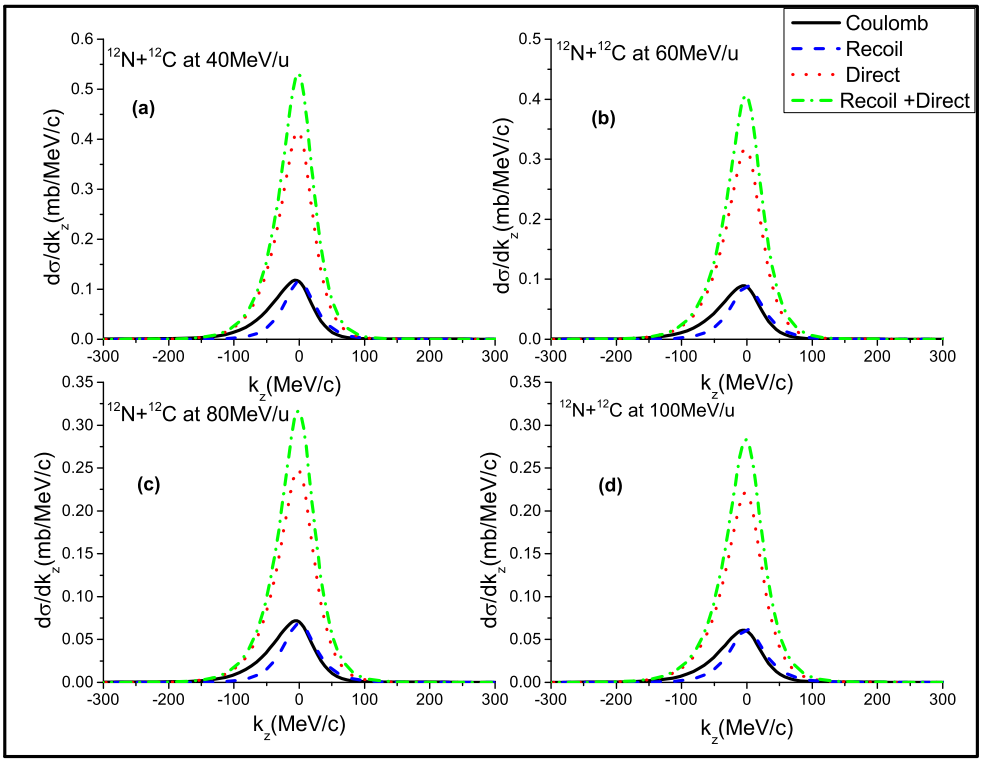

Fig. 3. LMD spectrum of the core fragment in the case of ^{12}C target at different energies showing the effect of the interference between the direct and Recoil Coulomb mechanisms. In each figure the black solid curve correspond to the total Coulomb mechanism, the blue dashed curve corresponds to the Recoil mechanism, the red dotted curve corresponds to the Direct mechanism, and the green dashed curve corresponds to the simple sum of the Recoil and Direct mechanisms

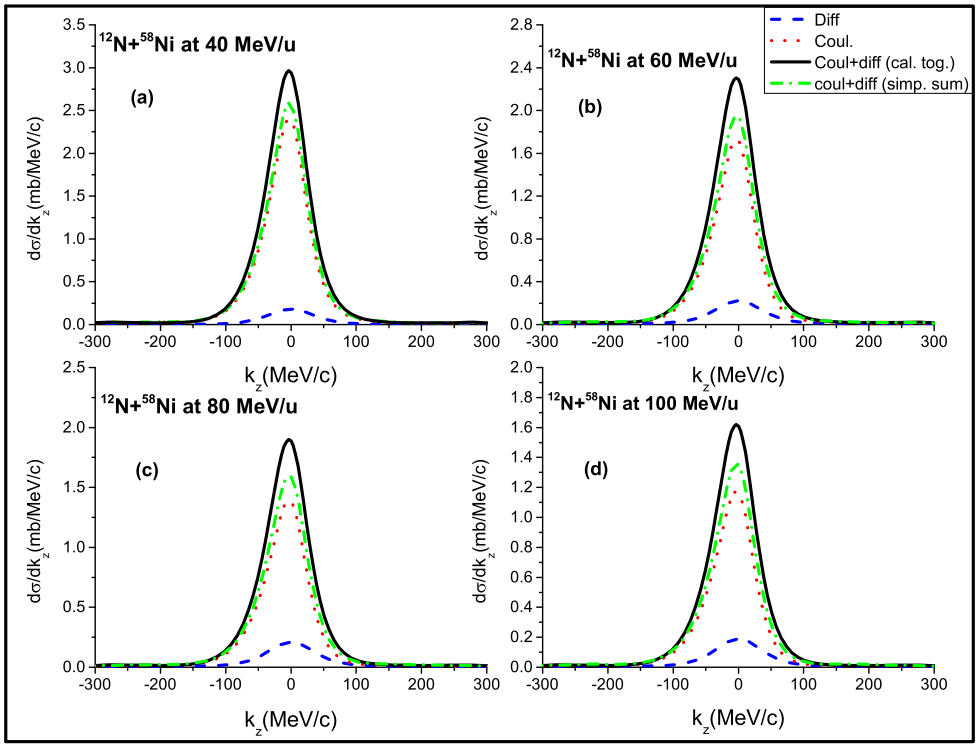

Fig. 4. same as Figure 2 but for ^{58}Ni target at different energies

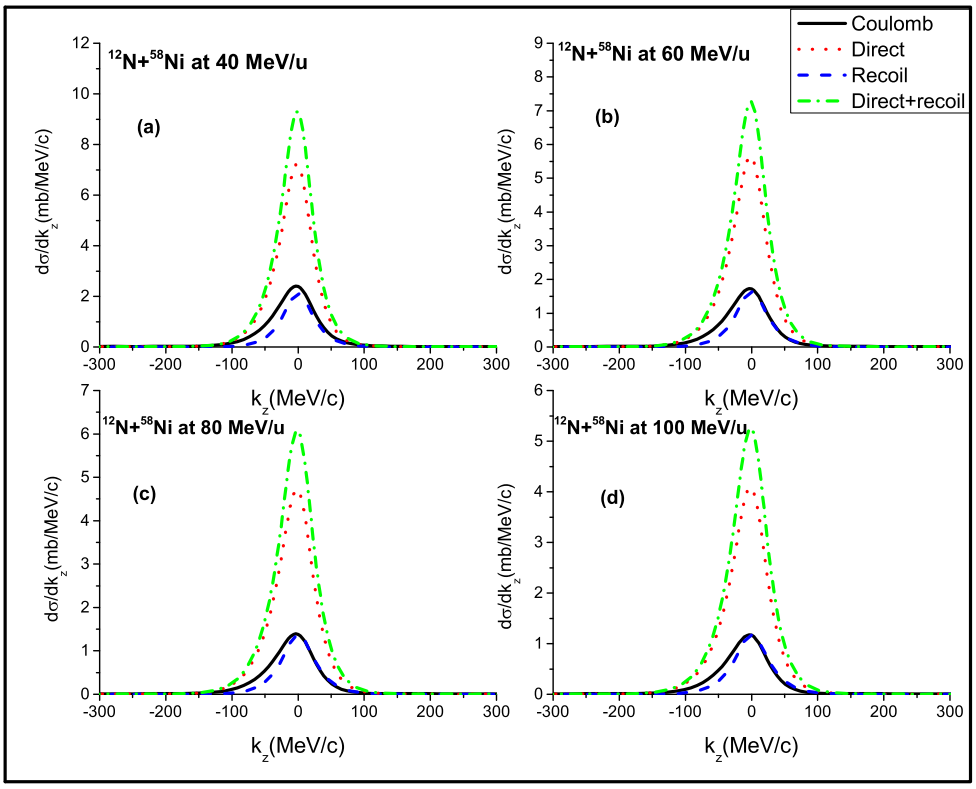

Fig. 5. Same as Figure 3 but for ^{58}Ni target at different energies

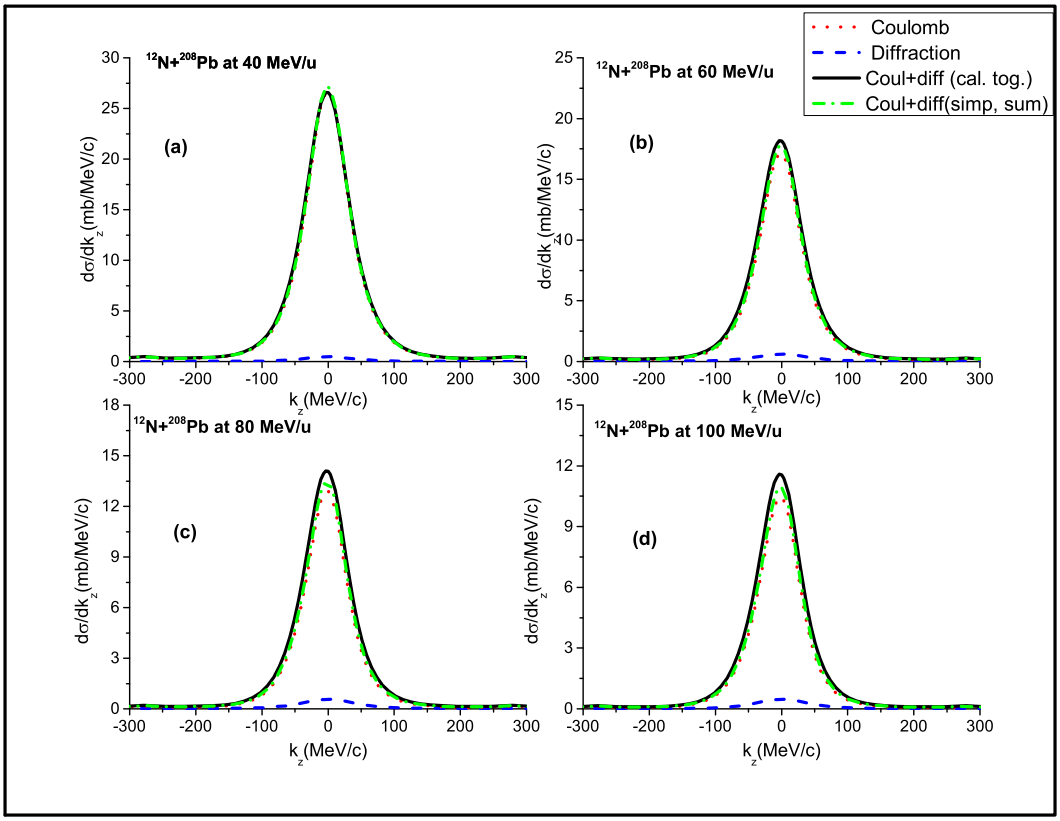

Fig. 6. Same as Figure 2 but for ^{208}Pb target at different energies

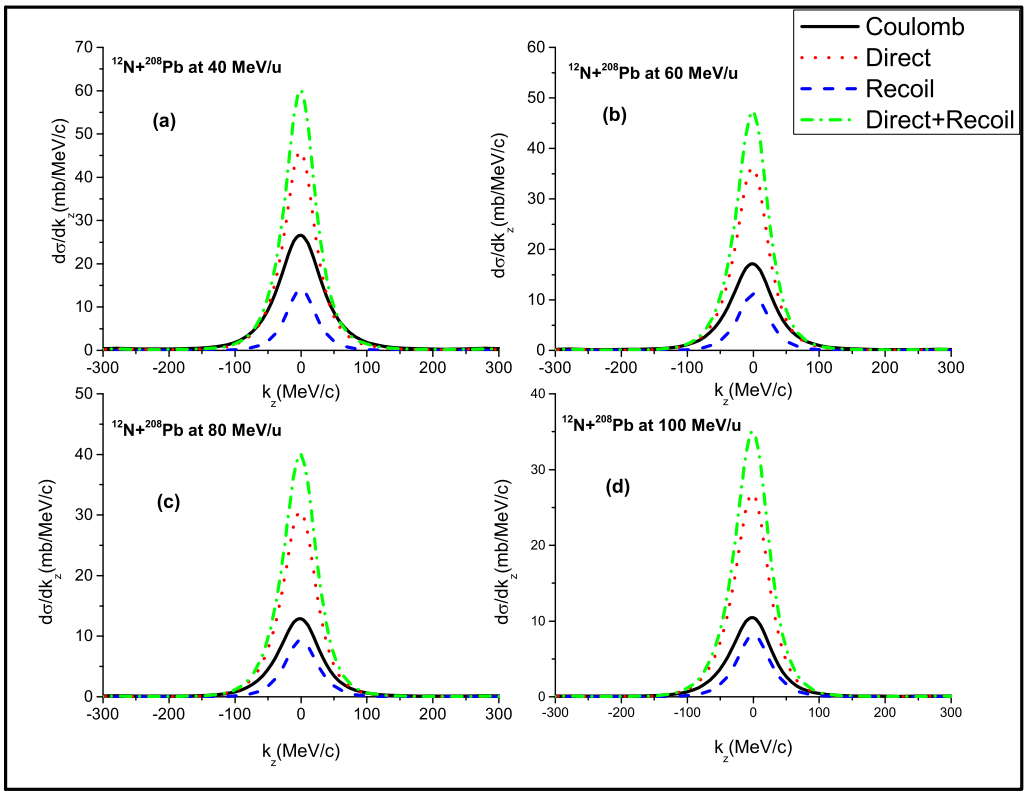

Fig. 7. Same as Figure 3 but for ^{208}Pb target at different energies

Beam Energy →	40 MeV/u	60 MeV/u	80 MeV/u	100 MeV/u
Breakup Mechanism	σ_{-p} (mb)	σ_{-p} (mb)	σ_{-p} (mb)	σ_{-p} (mb)
Diffraction	56	78	72	57
Coulomb	2539	1565	1150	917
Coul + Diff (simple sum)	2595	1644	1222	974
Coul + Diff (cal. togh.)	2642	1760	1341	1080
% Interference	+1.77%	+7.12%	+9.73%	+10.98%
Recoil	876	723	630	564
Direct	3207	2540	2189	1953
Recoil + Direct (simple sum)	4088	3262	2819	2516
Recoil + Direct (cal. togh.)	2539	1565	1150	917
% Interference	−36.50%	−52.02%	−59.21%	−63.56%

Table 5. Calculated single proton breakup cross-section (σ_{-p} in mb) for ^{12}N projectile on ^{208}Pb target at different incident beam energies corresponding to diffraction, Coulomb, and diffraction with Coulomb mechanisms, along with their percentage interference effects

Similarly, for heavy target ^{208}Pb case, the calculated single proton breakup cross-sections are shown in Table 5. It is clearly seen from Table 5 that the single proton breakup cross-section increases in the range of 1 to 10%, which shows a constructive nature of the interference. However, due to Recoil and Direct interference, it decreases in the range from 26 to 64%, showing destructive interference. Similarly, the interference effect on LMD width can be seen in Table 6. It is found that FWHM of LMD width increases 4 to 5% for all the incident energies for the Coulomb nuclear diffraction interference, while this enhancement in magnitude of LMD width due to Recoil and Direct interference lies within 38–19%. But here the enhancement is decreasing with an increase in beam energy. For better clarity, the LMD spectrums corresponding to each breakup mechanism and incident energy are shown in Figs. 6 and 7.

Beam Energy →	40 MeV/u	60 MeV/u	80 MeV/u	100 MeV/u
Breakup Mechanism	FWHM (MeV/c)	FWHM (MeV/c)	FWHM (MeV/c)	FWHM (MeV/c)
Diffraction	89.77	96.15	95.30	91.81
Coulomb	75.58	73.08	72.06	71.54
Coul + Diff (simple sum)	75.81	73.73	72.89	72.31
Coul + Diff (cal. togh.)	79.25	77.83	77.08	76.03
% Interference	+4.54%	+5.56%	+5.75%	+5.14%
Recoil	52.12	54.63	56.50	58.06
Direct	55.36	57.41	59.22	60.60
Recoil + Direct (simple sum)	54.48	56.71	58.56	59.96
Recoil + Direct (cal. togh.)	75.58	73.08	72.06	71.54
% Interference	+38.74%	+28.88%	+23.05%	+19.31%

Table 6. Calculated FWHM of LMD of the core fragment for ^{208}Pb target at different incident beam energies corresponding to diffraction, Coulomb, and diffraction with Coulomb mechanisms, along with their percentage interference effects

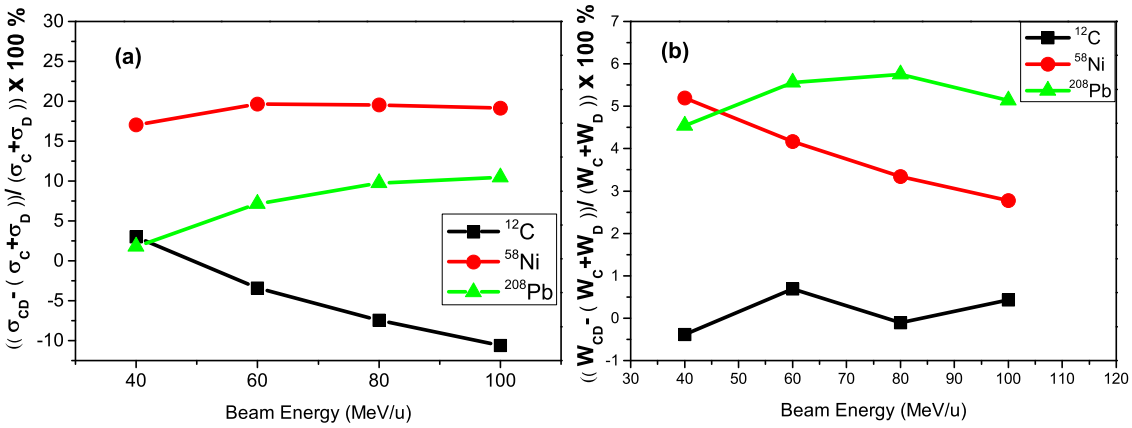

Fig. 8. Variation in magnitudes of (a) single proton breakup cross-section (σ_{-p}) (b) FWHM width of LMD, due to Coulomb nuclear diffraction interference with different target and incident beam energy.

From the above results (Fig. 8), we found that the variation in absolute magnitudes of a single proton breakup cross-section and FWHM of LMD width due to the Coulomb nuclear diffraction interference differs from each other and quantitatively, in terms, of percentage variation, depends on the target atomic number as well as on the incident beam energy. From Fig. 8, it is quite clear that interference effects are more pronounced in the case of ^{58}Ni target (medium size target) which can enhance the single proton breakup cross-section up to 20%, while the FWHM varies up to 5%. The obtained results are consistent with the results of Refs. [16, 30, 31, 45–48]. This constructive or destructive behavior of interference in the breakup reactions is complicate, particularly for the proton halo nucleus breakup reaction. This complexity may be understood via the projectile target optical potential, i.e. the imaginary part of optical potential contributes to the absorption that influences the breakup process. Meanwhile, the real part of optical potential modulates overall the interaction strength between the projectile and the target. For light targets, the dominance of the nuclear interaction enhances the role of the imaginary part, while in heavy targets cases, the Coulomb interaction predominantly contributes to and suppresses the significance of the real part. While in medium targets, the balance between these interactions creates conditions where both components of the optical potential play a vital role, leading to more pronounced interference effects.

The obtained results demonstrate that the Coulomb nuclear diffraction interference effects strongly affect the absolute magnitudes of breakup observables. Hence sufficient attention is highly required while dealing with the single nucleon breakup reactions, and we believe that this kind of study improves the clarity in the understanding of breakup reactions and interpretation of experimental results, which have profound application in astrophysical chain reactions.

IV. CONCLUSIONS

We have quantitatively investigated the effect of the Coulomb nuclear diffraction interference in single-proton removal from ^{12}N nucleus for ^{12}C, ^{58}Ni, and ^{208}Pb targets. This investigation is performed for the frequently used incident beam energy range, i.e. 40–100 MeV/u. We quantitatilvey analyzed the effect in terms of percent changes in the absolute magnitudes of a single proton breakup cross-section and FWHM of LMD, which are generally measured in exotic nuclei breakup reactions. We calculated the magnitudes of these observables by treating the Coulomb and nuclear diffraction breakup mechanisms independently and calculated their contributions in the absence of each other and together as well. The Coulomb and nuclear diffraction potential are treated with all order in sudden approximation within an eikonal like framework [28, 29, 45]. Further, the significance of Recoil and Direct Coulomb mechanism was studied in the light of ref [28, 29, 46–48]. We found that in ^{12}N nucleus breakup reaction, due to the Coulomb nuclear diffraction interference, the magnitude of single proton removal cross-section, for ^{12}C target, changes from 3–10% depending on the incident beam energy. On the other hand, for heavier ^{208}Pb target, the cross-section magnitude changes by 1–10%, depending on the incident energy. While for a medium mass target, i.e.^{58}Ni target, the variation in the breakup cross-section is 17–19%, depending on the incident beam energy. Regarding the effect on FWHM of the LMD width, it is found that the interference affects the magnitude of LMD width less than 1% for the ^{12}C target, 2–5% for the ^{58}Ni target, and approximately 5% for the ^{208}Pb target. This variation is found negligibly sensitive to the incident beam energy. On the other hand, the interference between direct and Recoil Coulomb mechanisms is affecting significantly both the breakup observable. So the interference behaves constructively or destructively depending on the target size and incident beam energy, and it is more difficult to predict for any breakup reaction with theoretical calculations. Thus, finally, we conclude that the Coulomb nuclear diffraction interference significantly affects the magnitude of these breakup observables, and it is more significant for a medium ^{58}Ni target in comparison with light and heavy targets. Therefore, it is important to consider this interference effects seriously, especially in a medium mass target reaction.

[1] I. Tanihata *et al.*, Phys. Lett. B **160** , 380 (1985); https://doi.org/10.1016/0370-2693(85)90005-X.

[2] I. Tanihata *et al.*, Phys. Rev. Lett. **55**, 2676 (1985); https://doi.org/10.1103/PhysRevLett.55.2676.

[3] T. Minamisono *et al.*, Phys. Rev. Lett. **69**, 2058 (1992); https://doi.org/10.1103/PhysRevLett.69.2058.

[4] W. Schwab *et al.*, Z. Phys. A **350**, 283 (1995); https://doi.org/10.1007/BF01291183.

[5] R. E. Warner *et al.*, Phys. Rev. C **52**, R1166 (1995); https://doi.org/10.1103/PhysRevC.52.R1166.

[6] F. Negoita *et al.*, Phys. Rev. C **54**, 1787 (1996); https://doi.org/10.1103/PhysRevC.54.1787.

[7] M. M. Obuti *et al.*, Nucl. Phys. A **609**, 74 (1996); https://doi.org/10.1016/0375-9474(96)00267-9.

[8] A. Navin *et al.*, Phys. Rev. Lett. **81**, 5089 (1998); https://doi.org/10.1103/PhysRevLett.81.5089.

[9] D. Pérez-Loureiro *et al.*, Phys. Rev. C **93**, 064320 (2016); https://doi.org/10.1103/PhysRevC.93.064320.

[10] D. D. Ni, Z. Z. Ren, Chin. Phys. C **41**, 114104 (2017); https://doi.org/10.1088/1674-1137/41/11/114104.

[11] X. Z. Cai *et al.*, Phys. Rev. C **65**, 024610 (2002); https://doi.org/10.1103/PhysRevC.65.024610.

[12] D. Q. Fang *et al.*, Phys. Rev. C **76**, 031601 (2007); https://doi.org/10.1103/PhysRevC.76.031601.

[13] A. Ozawa *et al.*, Phys. Rev. C **74**, 021301 (2006); https://doi.org/10.1103/PhysRevC.74.021301.

[14] T. Nagatomo *et al.*, Hyperfine Interact. **198**, 103 (2010); https://doi.org/10.1007/s10751-010-0262-8.

[15] A. Banu *et al.*, Phys. Rev. C **84**, 015803 (2011); https://doi.org/10.1103/PhysRevC.84.015803.

[16] R. Kumar, A. Bonaccorso, Phys. Rev. C **86**, 061601 (2012); https://doi.org/10.1103/PhysRevC.86.061601.

[17] P. Descouvemont, I. Baraffe, Nucl. Phys. A **514**, 66 (1990); https://doi.org/10.1016/0375-9474(90)90332-G.

[18] D. W. Lee *et al.*, J. Phys. G **38**, 075201 (2011); https://doi.org/10.1088/0954-3899/38/7/075201.

[19] B. Guo, Z. H. Li, W. P. Liu, X. X. Bai, J. Phys. G **34**, 103 (2006); https://doi.org/10.1088/0954-3899/34/1/006.

[20] X. Tang,*et al.*, Phys. Rev. C **67**, 015804 (2003); https://doi.org/10.1103/PhysRevC.67.015804.

[21] T. Q. Liu *et al.*, Phys. Rev. C **109**, 064604 (2024); https://doi.org/10.1103/PhysRevC.109.064604.

[22] H. Sadeghi, M. Ghambari, R. Fereidonnejad, Phys. Atom. Nucl. **79**, 55 (2016); https://doi.org/10.1134/S1063778816010166.

[23] N. Fukuda *et al.*, Phys. Rev. C **70**, 054606 (2004); https://doi.org/10.1103/PhysRevC.70.054606.

[24] A. Bonaccorso, D. M. Brink, C. A. Bertulani, Phys. Rev. C **69**, 024615 (2004); https://doi.org/10.1103/PhysRevC.69.024615.

[25] T. Nakamura *et al.*, Nucl. Phys. A **722**, C301 (2003); https://doi.org/10.1016/S0375-9474(03)01381-2.

[26] V. Guimaraes *et al.*, Phys. Rev. C **61**, 064609 (2000); https://doi.org/10.1103/PhysRevC.61.064609.

[27] R. Chatterjee, Phys. Rev. C **75**, 064604 (2007); https://doi.org/10.1103/PhysRevC.75.064604.

[28] A. García-Camacho, A. Bonaccorso, D. M. Brink, Nucl. Phys. A **776**, 118 (2006); https://doi.org/10.1016/j.nuclphysa.2006.07.033.

[29] Phys. Rev. C **76**, 014607 (2007); https://doi.org/10.1103/PhysRevC.76.014607.

[30] R. Kumar, A. Bonaccorso, A. Bonaccorso, Phys. Rev. C **84**, 014613 (2011); https://doi.org/10.1103/Phys

RevC.84.014613.
[31] Surender, R. Kumar, Proc. DAE-BRNS Symp. Nucl. Phys. **65**, 447 (2021); http://sympnp.org/proceedings/65/B122.pdf.
[32] J. Margueron, A. Bonaccorso, D. M. Brink, Nucl. Phys. A **703**, 105 (2002); https://doi.org/10.1016/S0375-9474(01)01336-7.
[33] V. S. Melezhik, D. Baye, Phys. Rev. C **59**, 3232 (1999); https://doi.org/10.1103/PhysRevC.59.3232.
[34] B. Mukeru, J. Lubian, L. Tomio, Phys. Rev. C **105**, 024603 (2022); https://doi.org/10.1103/PhysRevC.105.024603.
[35] M. Fukuda *et al.*, JPS Conf. Proc. **6**, 030103 (2015); https://doi.org/10.7566/JPSCP.6.030103.
[36] R. E. Warner *et al.*, Phys. Rev. C **74**, 014605 (2006); https://doi.org/10.1103/PhysRevC.74.014605.
[37] L. G. Sobotka *et al.*, Phys. Rev. C **87**, 054329 (2013); https://doi.org/10.1103/PhysRevC.87.054329.
[38] A. Lefebvre *et al.*, Nucl. Phys. A **592**, 69 (1995); https://doi.org/10.1016/0375-9474(95)00291-8.
[39] A. N. Danilov, A. S. Demyanova, A. A. Ogloblin, S. A. Goncharov, T. L. Belyaeva, in *Exotic Nuclei: Proc. International Symposium on Exotic Nuclei, 2020*, p. 17; https://doi.org/10.1142/9789811209451_0003.
[40] A. N. Danilov *et al.*, in *Proc. 13th International Conference on Nucleus–Nucleus Collisions, 2020*, p. 010031; https://doi.org/10.7566/JPSCP.32.010031.
[41] A. Galindo-Uribarri *et al.*, AIP Conf. Proc. **656**, 323 (2003); https://doi.org/10.1063/1.1556660.
[42] A. S. Demyanova *et al.*, JETP Lett. **111**, 409 (2020); https://doi.org/10.1134/S0021364020080020.
[43] J. X. Li *et al.*, Chin. Phys. Lett. **27**, 032501 (2010); https://doi.org/10.1088/0256-307X/27/3/032501.
[44] J. X. Li *et al.*, Chin. Phys. C **34**, 452 (2010); https://doi.org/10.1088/1674-1137/34/4/006.
[45] J. Margueron, A. Bonaccorso, D. M. Brink, Nucl. Phys. A **720**, 337 (2003); https://doi.org/10.1016/S0375-9474(03)01092-3.
[46] Surender, R. Kumar, Acta Phys. Pol. B **54**, 9-A1 (2023); https://doi.org/10.5506/APhysPolB.54.9-A1.
[47] Surender, R. Kumar, East Eur. J. Phys. No. 4, 200 (2024); https://doi.org/10.26565/2312-4334-2024-4-19.
[48] Surender, R. Kumar, Indian J. Pure Appl. Phys. **63**, 40 (2025).
[49] S. Goriely, M. Samyn, J. M. Pearson, Phys. Rev. C **75**, 064312 (2007); https://doi.org/10.1103/PhysRevC.75.064312.
[50] I. Angeli, At. Data Nucl. Data Tables **87**, 185 (2004); https://doi.org/10.1016/j.adt.2004.04.002.
[51] G. Audi, A. H. Wapstra, C. Thibault, Nucl. Phys. A **729**, 337 (2002); https://doi.org/10.1016/j.nuclphysa.2003.11.003.
[52] C. A. Bertulani, A. Gade, Comput. Phys. Commun. **175**, 372 (2006); https://doi.org/10.1016/j.cpc.2006.04.006.

ДОСЛІДЖЕННЯ КУЛОНІВСЬКОЇ ЯДЕРНОЇ ІНТЕРФЕРЕНЦІЇ В РЕАКЦІЇ РОЗПАДУ ЯДРА ^{12}N

Сурендер Каліраман, Равіндер Кумар
Науково-технічний університет імені Дінбандху Чхоту Рама, Муртал (Соніпат), Гар'яна, 131039, Індія

Досліджено вплив кулон-ядерної інтерференції на поперечний переріз відриву одного протона та ширину на половині висоти (FWHM) поздовжнього розподілу імпульсу (LMD) в реакції розпаду ^{12}N з трьома різними мішенями: легкими, середніми та важкими ядрами (^{12}C, ^{58}Ni and ^{208}Pb), за енергій пучка від 40 до 100 МеВ/нуклон. Використовуючи напівкласичний підхід, кулонівський розпад розраховано за допомогою раптового наближення в усіх порядках, тоді як ядерний розпад моделювали відомим еікональним наближенням у межах моделі Ґлаубера. Наші результати показують, що інтерференція суттєво змінює поперечний переріз розпаду для мішеней середньої маси. Проте FWHM LMD змінюється менш ніж на 6% для всіх типів мішеней. Отже, для мішеней середньої маси за будь-яких енергій пучка важливо враховувати інтерференцію між кулонівськими та дифракційними процесами розпаду. Це розуміння буде цінним для майбутніх експериментальних досліджень структури гало-ядер.

Ключові слова: гало-ядра, реакція розпаду, ефект інтерференції, поперечний переріз видалення одного протона.